Easterly Wave Disturbances Activity Over the Eastern Northeast Brazil During 2006-2010 Rainy Seasons

Acción de los disturbios ondulantes del este en el este del noreste de Brasil durante los períodos lluviosos de 2006 a 2010

Atuação dos distúrbios ondulatórios de leste sobre o leste do nordeste do Brasil durante os períodos chuvosos de 2006 a 2010

Bruce Francisco Pontes da Silva[1]
Rosmeri Porfírio da Rocha[2]
Helber Barros Gomes[3]

Abstract: Year after year, serious damages and financial losses have been caused by the intense rains associated with the Eastern Wave Disturbances (EWD) during the rainy season in eastern Northeast Brazil (ENEB). In order to contribute to the construction of methods capable of predicting EWDs more effectively, also allowing timely weather warnings to be issued to society, this study seeks to quantify the contribution of EWD during the ENEB rainy season and characterize their average synoptic processes for the period from 2006 to 2010. EWDs were identified through satellite images, streamlines, relative vorticity and divergence from the ERA-Interim reanalysis. On average, 23 EWD/rainy season were identified, representing 50-70% of the total precipitation.

Key-words: Easterly Wave Disturbances, composites, precipitation, wind, eastern part of Northeast Brazil.

Resumen: Año tras año, las intensas lluvias asociadas a los Disturbios Ondulantes del Este (EWD) durante la temporada de lluvias en el este de noreste de Brasil (ENEB) han causado graves daños

[1] Graduated in meteorology from the Institute of Atmospheric Sciences at the Federal University of Alagoas (ICAT/UFAL) and a master's degree in the same area from the Institute of Astronomy, Geophysics and Atmospheric Sciences at the University from São Paulo (IAG/USP). From 2012 to early 2020, he worked in research and operation in meteorology/agrometeorology at the Capixaba Institute for Research, Technical Assistance and Rural Extension (Incaper). Since March 2020, he was assigned to Cepdec/CBMES (Espírito Santo State civil defense). E-mail: bruce.silva@bombeiros.es.gov.br. Orcid: 0000-0002-2014-6782.

[2] BSc and MSc in Meteorology at University of São Paulo (USP) and Doctor in Meteorology from the National Institute of Spatial Research (Inpe). Currently holds the position of Professor on USP. E-mail: rosmerir@model.iag.usp.br. Orcid: 0000-0003-3378-393X.

[3] BSc in Meteorology at Federal University of Alagoas (Ufal) in 2005, MSc in Meteorology at University of São Paulo (USP) in 2008 and Doctor in Meteorology also from USP in 2012. Currently holds the position of Adjunct Professor on Ufal in the Institute of Atmospheric Sciences (Icat/Ufal). E-mail: helber.gomes@icat.ufal.br. ORCID: 0000-0001-9972-9990.

y prejuicio financiero. Con el fin de contribuir a la construcción de métodos capaces de predecir las EWD de manera más efectiva, permitiendo también la emisión de alertas meteorológicas oportunas a la sociedad, este estudio busca cuantificar la contribución de los EWD durante la temporada de lluvias de la ENEB y caracterizar sus procesos sinópticos promedio para el período de 2006 a 2010. Los EWD se identificaron mediante imágenes de satélite, líneas de corriente, vorticidad relativa y divergencia del reanálisis ERA-Interim. En promedio, se identificaron 23 EWD/temporada de lluvias, lo que representa 50-70% de la lluvia total.
Palabras-llave: Disturbios Ondulantes del Este, composiciones, precipitación, viento, este del noreste de Brasil.

Resumo: Ano após ano, sérios danos e prejuízos têm sido causados pelas chuvas intensas associadas aos Distúrbios Ondulatórios de Leste (EWD) durante a quadra chuvosa do leste do Nordeste do Brasil (ENEB). Com o fim de contribuir na construção de métodos capazes de prognosticar os EWD com maior eficácia, também permitindo emitir avisos meteorológicos em tempo hábil à sociedade, este estudo procura quantificar a contribuição dos EWD durante o período chuvoso do ENEB e caracterizar os seus processos sinóticos médios para o período de 2006 a 2010. Os EWD foram identificados via imagens de satélite, linhas de corrente, vorticidade relativa e divergência da reanálise ERA-Interim. Em média, foram identificados 23 EWD/quadra chuvosa, representando 50-70% da precipitação total.
Palavras-chave: Distúrbios Ondulatórios de Leste, composições, precipitação, vento, leste do Nordeste do Brasil.

1. Introduction

The Easterly Waves (EWs) are one of the most important weather systems to the total rainfall over many tropical regions. They can be defined as synoptic disturbances associated with troughs and warm sea surface temperature (Riehl 1945; Rosenthal 1960; Yanai 1963 1968; Krishnamurti and Baumhefner 1966; Williams 1970; Keshavamurty 1971; Reed and Recker 1971; Burpee 1974; Chang and Miller III 1977; Tai and Ogura 1987; Chou 1990; Asnani 1993; Espinoza 1996; Mota and Gandu 1997, 1998; Céron and Guérémy 1999). Most of the cases, the EWs signature is found in the lower and medium troposphere troughs (~850-700 hPa) associated with convective cloudiness moving from east to west over the tropical oceans, reaching inland areas

such as the Eastern Northeast Brazil (ENEB; Neiva 1975; Yamazaki and Rao 1977).

Some tropical meteorological systems genesis and development over Tropical South Atlantic (TSA) Ocean next ENEB are still not clear. It is hard to find the exact patterns that show how strong these systems are and when they will appear (Pontes Da Silva, 2008). There is a gap, especially with respect to the supposed Easterly Waves propagating over the TSA.

However, one can say the follow about the EWs genesis main causes, according to some researchers: 1) EWs may appear due the trade winds convergence (between the northeast and southeast trades or convergence along the northern or southern trade own flow); 2) EWs may develop due the intensification of a High Level Cyclonic Vortex to middle or low levels, spreading westward or 3) the EWs may develop due a mid-latitude trough displacement to the equator (frontal troughs that would detach from their fronts, heading west alongside the trades) or due an equatorial trough displacement to higher latitudes (may be associated with the equatorial trough) (Yamazaki and Rao 1977; Asnani 1993; Espinoza 1996; Fedorova 2008).

According to Asnani (1993), the greatest difficulties found in the EWs researches are: a) relatively low intensity: EWs are short compared to troughs and stationary ridges over tropical latitudes and cannot be identified in ordinary synoptic charts; b) lack of a homogeneous structure: the EWs are in the zonal current, and this current exhibits different characteristics in each Earth location, which in turn show different structures at each region; if the eastward flow is shallow (only low levels), shallow EWs are expected, but in a deeper eastward current (up to middle or high levels), deeper EWs are expected and c) few data available at the tropics: much of the tropical areas is covered by oceans, where it is difficult to install and operate meteorological stations.

Even over the continents, the density of meteorological stations is limited. In the meantime, satellites have provided data for areas remote areas such deserts and oceans. Even with this problem, many EWs searches were made. Many authors analyzed EWs through case studies by synoptic charts (Riehl 1945; Yanai 1963, 1968), through composites (Williams 1970; Reed and Recker 1971; Burpee 1975; Mota and Gandu 1997, 1998), using spectral analysis (Rosenthal 1960; Keshavururty 1971; Chou 1990), using orthogonal empirical functions (Espinoza 1996; Céron and Guérémy 1999) and also through dynamic simulations (Krishnamurti and Baumhefner 1966).

Specifically about cloudiness, Merritt (1964) found five different distributions of cloudiness associated with tropical disturbances, showing that not all EWs have convective cloud bands at synoptic scale. Many times, these systems only contain mesoscale shallow clouds during

some period, displaying convective clouds at another period. According to Merrit (1964), some EWs have no significant cloud cover at any stage of their life cycle but it does not mean that they are necessarily weak disturbances in the synoptic fields. Still, EWs usually have a cloudiness characteristic area standing out of other systems. This cloudiness may be predominantly stratiform or cumuliform, depending on the environment in which the waves are propagating. According to Asnani (1993), cloudiness and precipitation associated with EWs are commonly mixed with the Intertropical Convergence Zone (ITCZ) cloudiness and rainfall.

The possible mechanisms of the African EWs formation and maintenance were discussed by Burpee (1972, 1974), Rennick (1976); Karyampudi and Carlson (1988), among others. Reed and Recker (1971), Keshavamurty (1971), Chang and Miller III (1977) and Tai and Ogura (1987) researched about the tropical Pacific Ocean EWs. Overall, the northern hemisphere EWs have wavelength of ~3000 km, 4-5 days period and 5 to 7° day^{-1} phase speeds (~7ms^{-1}) as Asnani (1993) concluded about the studies available till the earlier 90's.

According to studies for the TSA, the EWs events occur at any time of the year, often influencing the ENEB (Chou 1990; Espinoza 1996). Its maximum frequency occurs in the austral autumn/winter (the ENEB rainy season) (Yamazaki and Rao 1977). Most of the time, these systems can be observed through satellite images as shallow clouds spreading from east into the ocean and intensifying next to the coast, forming convective clouds (Molion and Bernardo 2000), but sometimes the EWs spreads to ENEB already with convective activity, weakening as they enter the continent.

Yamazaki (1975) conducted a theoretical study on barotropic instability in the eastern zonal current of the TSA and ENEB, which may be directly related to the origin and maintenance of EWs. The study of barotropic instability obtained a wavelength of ~6000 km. The author verified the results of this theory observing the cloudiness that was spreading over the TSA, concluding that the disturbances propagate only in the austral winter with wavelength of 4000 km, concluding that this result (observed) is in agreement with the theoretical result. In the range between latitudes 5° and 10°S, Yamazaki noted the spread to the west of well-defined aligned clouds, from the longitude of 10°E to approximately 40°W. Chou (1990) showed that the fall and winter 1979 EWs presented wavelength of 6200 km. Espinoza (1996) summarized in a table information on several studies on EWs (in several regions of the globe), besides studying them through data of the southern component of the wind for a period of 10 years (1980-1989). That author noted that the TSA EWs

spread all year round with different wavelengths: in the austral summer, the observed wavelength ranged from 6000 to 7000 km, but in the austral fall, the length was from 5000 to 6000 km. In the austral winter, the waves were shorter, with lengths ranging from 3500 to 4000 km. Torres (2008) studied some EWs that moved to ENEB in its 2005 and 2006 rainy seasons. Torres found 26 EWs, with wavelength of 4000 km. The author used satellite data and Hovmöller-type diagrams and found that the EWs amplitude increased gradually from April to July (ENEB rainy season), indicating a possible existence of a well-defined seasonal cycle for EWs, that is, a seasonal progressive increase in the number of EWs. Gomes et al. (2015) analyzed the circulation associated with the propagation of easterly wave disturbances (EWDs) in the ENEB rainy season from 2006 and 2007 (April to July), based on the cases identified by Pontes da Silva (2011). The composite fields of 700 hPa showed a wavelength of 4500 km. These results are according to Pontes da Silva (2011), who found an average wavelength of 4306.8 km, measured by compositions for the EWDs detected between 2006 and 2010 during the rainy season of the ENEB. According to Pontes da Silva (2011), the EWDs contributed at least with 70% of the total precipitation observed over the ENEB during the rainy seasons of 2006 to 2010.

Yamazaki (1975) also observed that the EWs presented a period of 4 days, concluding that the high precipitation amounts observed in the austral winter on the ENEB is associated with EWs (Yamazaki and Rao 1977). Kayano (1979) verified that the EWs spread to the Amazon having a period of 3 to 5 days and maximum humidity next to the EWs trough. Chou (1990) observed that EWs that reached ENEB (5°S) in the year 1979 had an average period of 5 to 6 days, Torres (2008) found a 5-day period between 2005 and 2006, Pontes da Silva (2011) observed a period of 5.3 days and Gomes et al. (2015) found a EWs period of 5.5 days.

About the EWs phase speed, Yamazaki (1975) found 10 $m.s^{-1}$, Espinoza (1996) verified 10 to 14 $m.s^{-1}$ at the austral summer and 10-13 $m.s^{-1}$ at the austral fall and winter. Chou (1990) verified phase velocity of 12 ms^{-1} at the 1979 fall and winter. Torres (2008) found a phase speed of 10 $m.s^{-1}$. Both Pontes da Silva (2011) and Gomes et al. (2015) found a EWs phase speed of 9.5 $m.s^{-1}$.

Summarizing the kinetic characteristics of the TSA EWDs' works, the waves have an averaged wavelength between 4000 and 6000 km, period of 5 days and phase speed around 10 ms^{-1}.

Some authors to propose that, depending on certain particularities, the eastern

perturbations in the TSA cannot be called Easterly Waves (Merritt 1964; Riehl 1979; Diedhiou et al. 2010). But, in this paper we do not discuss the existence or not of "classic" EWs over the TSA. However, we will be referring to the waves in the trades found over the TSA and reaching the ENEB in its rainy season as *Easterly Wave Disturbances* (EWDs), as Pontes da Silva (2011) did. More recently, Gomes et al. (2019) used the same methods applied in this study (based on Pontes da Silva (2011)) to identify EWDs for a longer period.

The ENEB is located in a highly vulnerable area to meteorological disturbances that propagate westward, which occur typically at tropical latitudes. Almost the entirely precipitation amount over the ENEB at its rainy season is caused by EWDs, convergence zones associated to cold fronts (FEs) or cold fronts (FSs) themselves (Kousky 1979, 1980; Molion and Bernardo 2002; Pontes Da Silva (2011); Kouadio et al. 2012). Those weather systems frequently interact with the sea-land and land-sea breezes. Heavy rainfall events are not common even during the ENEB rainy season in areas from 100-250 km inland from the coast.

The objective of this study was to verify the TSA EWDs average propagation characterists and precipitation contribution over the ENEB rainy season through events' composition. For this, a detailed synoptic analysis was performed to identify the EWDs' events that reached ENEB in its rainy seasons from 2006 to 2010.

2. Data and Methodology

2.1 Data

The EWDs precipitation was characterized through the Tropical Rainfall Measuring Mission (TRMM; Huffman et al., 2007) dataset. This data is obtained by an algorithm called 3B-42, which aims to produce rainfall analysis by combining high quality infrared and microwave observations considering their mean square errors evaluations.

The atmospheric variables (zonal and meridional winds (u, v), relative humidity (RH), outgoing longwave radiation (OLR) and pseudo-vertical velocity (omega - ω) are provided by the ERA-Interim (ECMWF - European Centre for Medium-Range Weather Forecasts Reanalysis Interim – ERAIN) reanalysis (Dee et al. 2011). This reanalysis is available from 1979 with 37 vertical levels and 1.5º of horizontal resolution.

All the satellite images (infrared channel; IR) from METEOSAT-7, 8 and 9 available were obtained from the GIBBS/NCDC/NESDISS/NOAA (Global ISCCP - International Satellite Cloud

Climatology Project - B1 Browse System/National Climatic Data Center/ National Environmental Satellite, Data, and Information Service/National Oceanic and Atmospheric Administration) database. Additional Meteosat-7 images with higher spatial resolution were provided by the Dundee Satellite Receiving Station (DSRS) University of Dundee.

All data were obtained within the period from 2006 to 2010.

2.2 Methodology

For AMJJ from 2006-2010 the EWDs were identified through synoptic analysis of the satellite imagery and meteorological fields. The EWDs basic synoptic environment and kinetic characteristics were obtained by composites.

The area of study is shown at figure 1b and the ENEB location is zoomed over figure 1a. That takes the TSA ocean, since Africa, and the northeastern Brazil, from 30 °E to 45 °W and between 10 °N and 40 °S (figure 1b). Some satellite images and meteorological fields were zoomed to better identify the synoptic systems along the analysis.

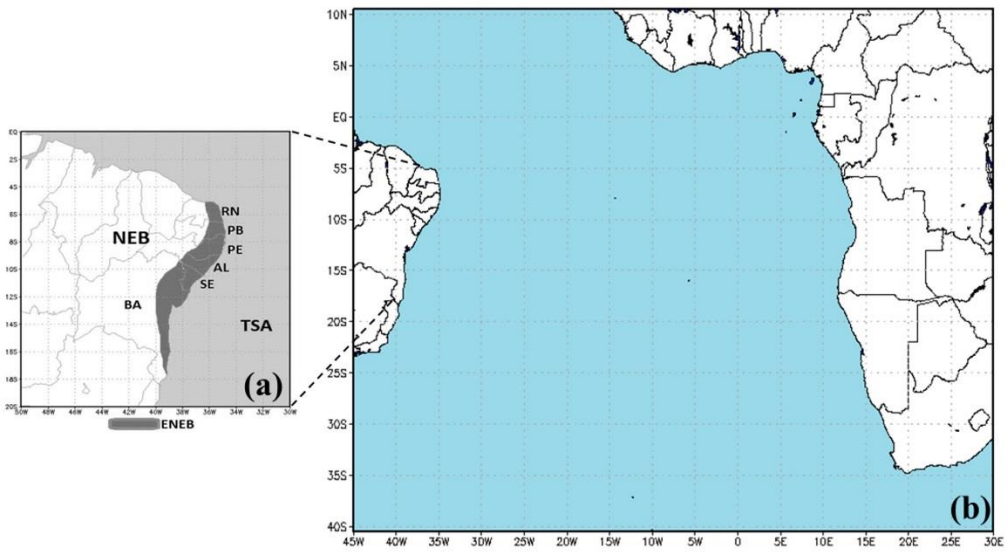

Fig. 1 Location of Northeast Brazil (NEB), eastern of NEB (ENEB, grey shading area) and part of the tropical South Atlantic Ocean (TSA) (a). Also are indicated the names of the states of ENEB: Rio Grande do Norte (RN), Paraiba (PB), Pernambuco (PE), Alagoas (AL), Sergipe (SE) and Bahia (BA). Domain used to search for EWDs in this research is found on b. The area covers the TSA, part of Africa and NEB.

The exact procedures to identify the EWDs were as follows:

1 – Identification by streamlines and relative vorticity:

a) Meso or synoptic troughs at 1000, 850, 700 hPa, not necessarily at all levels at the same time, but at least at 850 and 700 hPa, moving from east and trough or at least easterly flow at 500 hPa seen by the streamlines. The 200 hPa level was analyzed to see if the flow was from east or west at high levels, but it was not given too great importance, since the EWDs are very week at higher levels.

b) At the same time, the cores of relative vorticity were tracked associated with the wind.

2 – Searching for nebulosity by satellite imagery:

The analysis of IR satellite imagery considered the cloudiness pattern which displaces westward over the tropical South Atlantic Ocean (TSA). The EWDs cloudiness characterization of Hall (1989) suggested the existence of four unique areas: 1) a ridge area associated with fair weather and high visibility, with surface divergent flow, subsidence and low cumulus (Cu) humilis clouds; 2) the region near the trough axis, where predominates developing Cu clouds, cirrus (Ci) and altocumulus (Ac) with reasonable visibility, however showing a sparse rainfall formation; 3) an area near the trough with the presence of Cu congestus, Ci and Ac and frequent rain and 4) the region behind the trough axis, with convergent flux and strong upward movement, presenting cumulonimbus (Cb) and moderate to intense precipitation.

In this study, the EWDs subjective identification occurred reversibly in many cases, i.e., by animating satellite images backward from the moment in which the wave is better characterized by the cloud cover with synoptic or sub-synoptic dimensions, including or not Cbs (rarely it was noticed total absence of Cbs). Because we are interested in the EWDs impact over ENEB (see gray area in Fig. 1), only the EWDs associated with clouds that have attained this area were considered.

A classic EWD detection by cloudiness example in the IR satellite imagery is presented in Figure 2. We can see initially the EWD low clouds cluster on 1500 UTC 05 and 1800 UTC 07 June 2007 (Figs. 2a-b). In the next days, there is the development of Cbs in the EWD area that is getting closer to ENEB on 1200 UTC 09 and 1800 UTC 11 June 2007 (Figs. 2c-d).

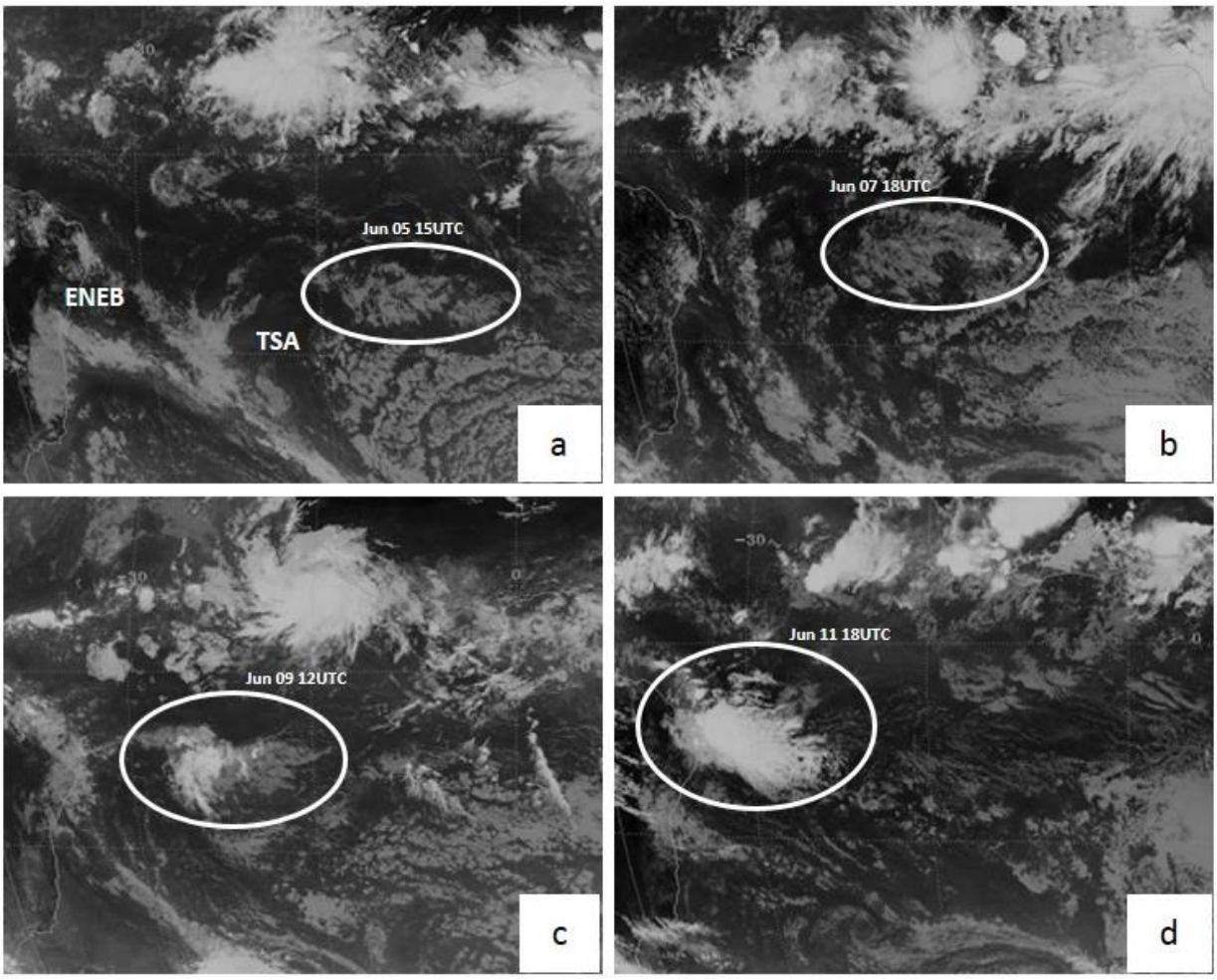

Fig. 2 Infrared channel satellite images from METEOSAT-9 at 1500 UTC 05 (a), at 1800 UTC 07 (b), at 1200 UTC 09 (c) and at 1800 UTC 11 (d) of June 2007. The ellipses indicate the cloudiness associated with the EWDs propagating over the TSA till its arrival in ENEB.

2.3 Hovmöller Diagrams

For each rainy season, meridional winds Hovmöller diagrams were constructed for the 0oW to 40°W longitude at 850 and 700 hPa. These longitudinal sections considered the meridional wind average between 1 and 10°S that was filtered using a low-pass filter. This filter was applied to eliminate the oscillations with certain periodicity, 3-7 days in the EWDs case.

2.4 EWDs Visual Verification in the Atmospheric Fields

After the first EWDs identification in the IR satellite images, a visual analysis of the streamlines and relative vorticity fields at different pressure levels (1000, 850, 700, 500 and 200 hPa) was performed to locate the troughs and cyclonic cores associated with the disturbances.

2.5 EWDs Composites

Composite fields are meant to show the gradual and progressive mean time evolution of a dataset, and such technique can be applied to atmospheric variables. In this study, we used composites to characterize the mean synoptic environment associated with EWDs. This allows identifying the favorable conditions to the EWDs development or intensification, as well as their weakening conditions.

The EWDs composites of atmospheric variables (wind, relative vorticity, horizontal divergence, omega, etc) considered 1200 UTC data (except for precipitation, which is available as daily totals) since three days before (day -3) until one day after (day +1), where the day 0 refers to the date when the EWDs are closer to the ENEB coastline. As will be shown, the EWDs intensify near ENEB and quickly decay after reaching the continent, having an average lifetime of five days and staying near ENEB at least 2-3 days. Therefore, the 5-day period used for this analysis can adequately characterize the EWDs synoptic environment. The composites for OLR and precipitation have considered the period from day -2 to day +2.

For the period of 2006-2010 AMJJ, the difference between the EWDs events composites and the fields mean was calculated and will be referred as anomaly. The statistical significance of the anomalies was accessed using the two-sided Student's t-test at 95% confidence level (Wilks 2006).

The 700 hPa streamlines composites were used to calculate the wavelength and period averages, and consequently the EWDs phase velocity. Besides, the statistics of the frontal systems (FSs) crossing Brazil, ITCZ positioning, precipitation and SST information were obtained from CPTEC/INPE monthly synoptic synthesis and INFOCLIMA webpages, while El Niño-Southern Oscillation (ENSO; Philander 1990) information was available at NOAA's ENSO webpage.

3. Results: EWDs Mean Characteristics, Composites and Anomalies

3.1 Hovmöller Diagrams

The EW trough was identified in the Hovmöller diagram by the 0 line, which marks the meridional wind changes from south (positive) to north (negative) in a given reference point. The reverse denotes ridge identification. Considering the EWDs identified by satellite images and atmospheric fields, it was found that the Hovmöller diagrams detected ~68.6% of these systems, indicating the limitation of this technique to analyze the EWDs. Therefore, Hovmöller diagrams

were not used here to calculate the EWDs kinematic characteristics, once the subjective identification of EWDs (as described in section 2) proved to be more accurate.

3.2 EWDs Mean Characteristics

For AMJJ from 2006-2010, 116 EWDs that reached ENEB were identified over TSA, resulting in an average of 23 EWDs cases per rainy season. Table 1 presents the main characteristics of the EWDs identified using satellite image and ERA-Interim reanalysis. The EWDs are more frequent over ENEB in June. On average, almost 60% of the EWDs occurred in each rainy season were associated with convective clouds, at least when interacting with the local circulations (sea and land breezes) near the ENEB coastline. This feature was also discussed in the observational study of Mota (1997). According to Table 1, the EWDs have an average lifetime of 5 days (from its first detection until the dissipation) with ±2 days of standard deviation, producing a mean of 2.6 rainy days over ENEB per event (standard deviation of ±1.5). Using the 700 hPa composite fields, EWDs average lifetime and wavelength are, respectively, 5.3 days and 4307 km. These results provide a mean EWDs phase velocity of 9.5 m s^{-1} that is similar to the values found by Mota (1997). Table 1 indicates that EWDs propagations affect more the eastern of PE and PB states, where the climatology of precipitation shows a peak during AMJJ.

Reference	2006	2007	2008	2009	2010	Total	%	Average
Total of EWs (AMJJ)	26	22	24	22	22	116		23.2
Presence of convective activity (at least moderately)	11	12	17	16	12	68	58.6	13.6
Number of events at April	6	5	5	5	6	27	23.3	5.4
Number of events at May	5	6	4	4	5	24	20.7	4.8
Number of events at June	7	5	9	7	5	33	28.5	6.6
Number of events at July	8	6	6	6	6	32	27.6	6.4
Mean duration (days)	4.8	5.0	5.4	6.4	4.5			5.2
Wavelength (km)	4773	4662	3996	3996	4107			4307
Phase Velocity (m s^{-1})	11.8	9.8	8.9	8.4	8.6			9.5
Period (days)	4.7	5.5	5.2	5.5	5.5			5.3
Most affected states (events total - satellite)	PB/PE	PB/PE	PB/PE	PB/PE	PB/PE			
Number of rainy days in ENEB due EWs	2.4	2.5	2.9	3.2	2.2			2.6

Table 1 Mean characteristics of EWDs identified in the period AMJJ from 2006-2010.

Using Era-Interim reanalysis and satellite images, the EWDs were associated with other synoptic systems acting over the TSA. On average, it was found that almost 30% of the EWDs are associated, in some stage of their lifetime, with FEs or FSs themselves (Table 2). This kind of tropical wave is generally formed by the trough release from a frontal zone extremity, which is

moving westward due to the trade winds. Besides, there is a weaker association between EWDs and ITCZ, i.e., the EWDs occur in 17% of the time when ITCZ is still close to the northern coast of northeast Brazil. Many times, the flow perturbations in the SASR (South Atlantic Subtropical Ridge/St. Helena High) due to the troughs propagation from western Africa does not mean that the SASR was directly connected to the EWDs, despite the fact that these waves propagate into the subtropical anticyclonic flow (Asnani 1993). It is important to remember that the high pressure systems central area is usually associated with fair weather, while its edges are often overshadowed by clouds. Typically for the Southern Hemisphere, the western/northwestern anticyclones edges have exactly this characteristic, despite of their migratory or subtropical nature (Fedorova 2008). Table 2 shows that no substantial pressure anomalies were observed in the SASR area associated with EWDs activity in the 2006-2010 periods.

Reference	2006	2007	2008	2009	2010	Total	%	Average
ENSO (AMJJ)	neutral	neutral	-	+ (MJJ)	+ (AM) - (JJ)			
Frontal Systems	4	5	5	1	3	18		3.6
ITCZ average positioning	**0**	+	**0**	-	+			
SST anomalies over TSA	+	**0**	+	+	+			
SASR surface presure anomalies	**0**	**0**	**0**	**0**	**0**			
ITCZ association	3	3	4	5	5	20	17	4
FS association	14	4	8	3	4	33	28	6,6
1000 hPa troughs association	15	12	18	15	15	75	64.7	15
1000 hPa confluence (except ITCZ)	11	12	14	14	12	63	54.3	12.6
700 hPa troughs association	21	20	22	21	19	103	88.8	20.6
850 hPa troughs association	20	21	20	20	17	98	84.5	19.6
500 hPa troughs association	9	12	14	12	7	54	46.6	10.8

Table 2 Association of EWDs with other systems: anomalies of surface pressure and sea surface temperature (SST), ENSO phase, frontal systems at the rainy season and ITCZ average positioning.

The 1000 hPa wind fields (Figs. not shown) indicate that almost 65% of the EWDs events have a trough practically stationary over ENEB (Table 2), probably related to the trade winds which turns cyclonically near ENEB coastline. Pontes da Silva (2008 and 2011) obtained that 51% of these troughs were connected to an observed rainfall rate greater than 5 mm day^{-1} between 2003 and 2006 over AL (located in the central part of ENEB as shown in Fig. 1), indicating that the cyclonic circulation in the trade winds is directly related to the moderate to intense precipitation in the region. The wind confluence occurs in almost half of the EWDs events at the 1000 hPa level (Table 2). This is important because some FEs may be identified by this circulation pattern and also because the confluence suggests convergence along the coast. The moisture flux convergence

was not analyzed, but the confluent and convergent wind patterns, summed with the availability of moisture over the TSA, suggest positive contribution of the 1000 hPa level to the EWDs intensification when they are approaching ENEB.

As at 1000 hPa, the 850 hPa level shows a cyclonic circulation pattern along ENEB and troughs moving to this area in ~84% of the EWDs events (Table 2). The presence of troughs is larger at 700 hPa where they are identified in ~90% of the EWDs (Table 2) moving almost in phase with the cloudiness. This suggests that this level defines better the synoptic circulation associated with EWDs, allowing the detection of almost all systems. When they are not identified at this level, a trough was present at another level. Therefore, the levels of 850 and 500 hPa are important by adding just a few more EWDs events to those identified at 700 hPa. Besides, a careful visual analysis shows that a large EWDs number may be detected by the cyclonic (negative) relative vorticity cores propagation.

On average, 3.6 cold fronts reached ENEB during AMJJ and were related to EWDs (Table 2). The ITCZ was farther north ("+" in Table 2) of its climatological position in both 2007 and 2010, southward ("-" in Table 2) in 2009 and near the climatology ("0" in Table 2) in 2006 and 2008. In Table 2 all the ENEB rainy season months (AMJJ) were considered, although the larger southward displacement of ITCZ over the northern Northeast Brazil is normally observed no much after May (Uvo and Nobre 1989).

The EWDs usually may generate severe tropical storms when they propagate over warmer waters, which can further develop into hurricanes (Shapiro 1977; Thorncroft and Hodges 2001). The analysis of the TSA EWDs and TSA SST association could show if there is a connection between the warm/cold SST anomalies and the EWDs development/maintenance in the region. However, this was not a purpose of the present study since in the 5 rainy seasons the SST anomalies were positive in all years ("+" in Table 2), except in 2007 when the SST was on average ("0" in Table 2).

Table 2 presents the signal of ENSO indexes for the months AMJJ obtained from NOAA (http://www.elnino.noaa.gov/). The AMJJ months of 2006 and 2007 years were characterized as ENSO by neutral phase, while it was negative ("-" in Table 2) in 2008. For 2009 ENSO index was positive ("+" in Table 2) in MJJ and in 2010 it changed from positive during April-May to negative in June-July. In terms of precipitation, it was observed during AMJJ from 2006 to 2010 weaker negative anomalies over ENEB, except in 2009 (Figs. not shown).

Figure 3 synthesizes the mean position of the areas where EWDs propagations are observed. In this figure the mean positions of the 700 hPa trough from day -3 until day 0 are also indicated. The EWDs reaching ENEB originate mainly westward of 20ºW, propagating westward and being near the coast at day 0. These results are in according with Berry et al. (1945) work made before the satellite era, which had already suggested that this region is favorable to the development and propagation of EWDs (see inset of Fig. 3).

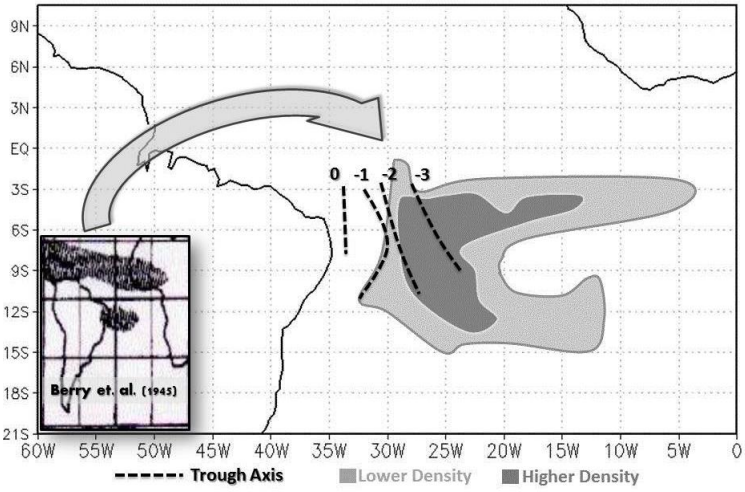

Fig. 3 Mean position of origin of EWDs according the infra-red satellite imagery (shaded, with scale of intensity in the bottom), mean location of 700 hPa EWDs troughs between days -3 and day 0 (thick dashed line). The inset indicates the areas affected or where existed EWDs evidence (shaded areas at the lower left of Figure) according to Berry et al. (1945).

3.3 EWDs Horizontal Structure: anomalies

The wind and relative vorticity anomaly fields are present in Figure 4. At 850 hPa a cyclonic core is already propagating over TSA (near 10ºS-25ºW) since day -3, but it is weaker than the core at 1000 hPa (Figs. 4a-e). Between days -2 and -1 the cyclonic core continues moving westward and an anticyclonic core intensification is observed upstream of the cyclonic core (Figs. 4g-h). This core intensifies on day 0, when it reaches ENEB, but its southern part is weakening (Fig. 4d). From day 0 to day +1, another cyclonic area is propagating between the longitudes 5-25°W (Figs. 4i-j). The anomalous winds show a cyclonic flow over ENEB on day 0, while the trough reached the region one day before (Figs. 4h-i).

At 700 hPa, the cyclonic anomalous core moved northwestward between days 0 and +1 (Figs. 4n-o), from 35°W to 42°W (as occurred at 850 hPa level), but it is less organized between days -3 and -1 due to the presence of an anticyclonic anomaly center upstream of the cyclonic core (Figs. 4k-m). Between days 0 and +1 the cyclonic cores reach ENEB (Figs. 4n-o). The anomalous

wind field suggests that the trough associated with EWDs advances in day -1 (Fig. 4m), and on day +1 there is another trough approaching ENEB (Fig. 4o).

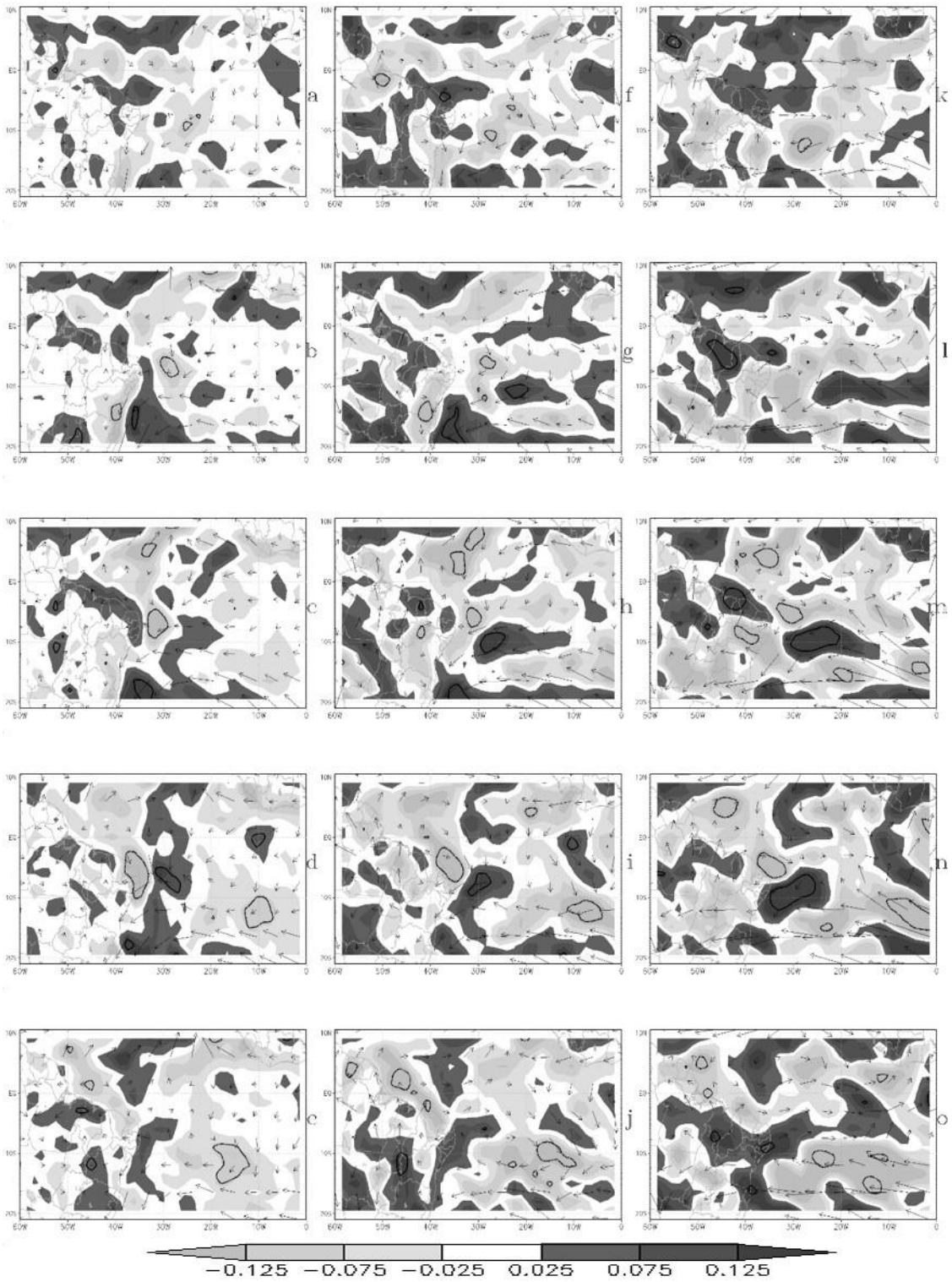

Fig. 4 Wind (m s-1, arrows) and relative vorticity (x10-5 s-1, shaded with scale at the bottom) anomalies due EWDs from day -3 (a, f, k), day -2 (b, g, l), day -1 (c, h, m), day 0 (d, i, n) and day +1 (e, j, o) at 1000 (a-e), 850 (f-j) and 700 hPa (k-o). The black line indicates the statistically significant anomalies at 90%.

The 500 hPa level analysis show noisy flow. In general, one can only say that at mid-levels the anticyclonic circulation tends to weaken over TSA. In the streamlines synoptic analysis, it is seen that the 500 hPa troughs are very broad, covering much of TSA. During EWDs the anomalous easterly winds predominate over eastern BA, indicating the weakening of westerly winds. In the 200 hPa vorticity and circulation anomaly fields the EWDs signal is not as clear as at low levels, but it is found that the wind tends to diverge under anomalous anticyclonic vorticity in day 0 over part of ENEB (Figs. not shown).

Some studies have shown that the EWDs propagation is associated with mass convergence and divergence, respectively, at low (1000/925hPa) and upper levels of the atmosphere (Reed et al. 1977). In the composites of this work the divergence is observed already at 850/700 hPa, while there is convergence at 1000 hPa. During the rainy season this convergence along the ENEB coast is typical and it is mainly attributed to the: (a) deceleration of southeasterly trade winds blowing perpendicular to the coast due to the large roughness over continent and (b) due to southeasterly trade winds convergence with the land breeze in the pre-dawn and early morning (Kousky 1979; da Rocha et al. 2009).

At 850 hPa, it is found a divergent pattern over ENEB due to the wind acceleration downstream of the trough. There is also divergence at the 700 hPa level, but it is in phase with the 1000 hPa convergence. This means that both are located in a coastal strip, with strongest signal on the TSA sector located immediately eastern of ENEB. At 500 hPa the divergence is weaker. Over southern and eastern BA the flow converges what does not favor the EWDs activity.

The divergence anomalies are more intense at low levels. In both 1000 and 850 hPa there is a convergent core near ENEB. At 1000 hPa, the convergence anomaly associated with EWDs is present already in day -3 far from shore (Fig. 5a) and it propagates westward intensifying from day -2 to day 0 (Fig. 5b-d), while at 850 hPa the intensification occurs from day -1 to day 0 (Fig. 5f). Above the anomalous convergent areas at 1000 hPa, the 700 hPa level anomalies show divergent core moving westward between day -1 and day 0 (Figs. 5l-n). At 500 hPa the convergence/divergence anomalies are weak (Figs. not shown), but the divergence intensifies at upper levels (200 hPa) on day 0. This vertical structure of the divergence suggests that the EWDs acting over TSA are predominantly shallow.

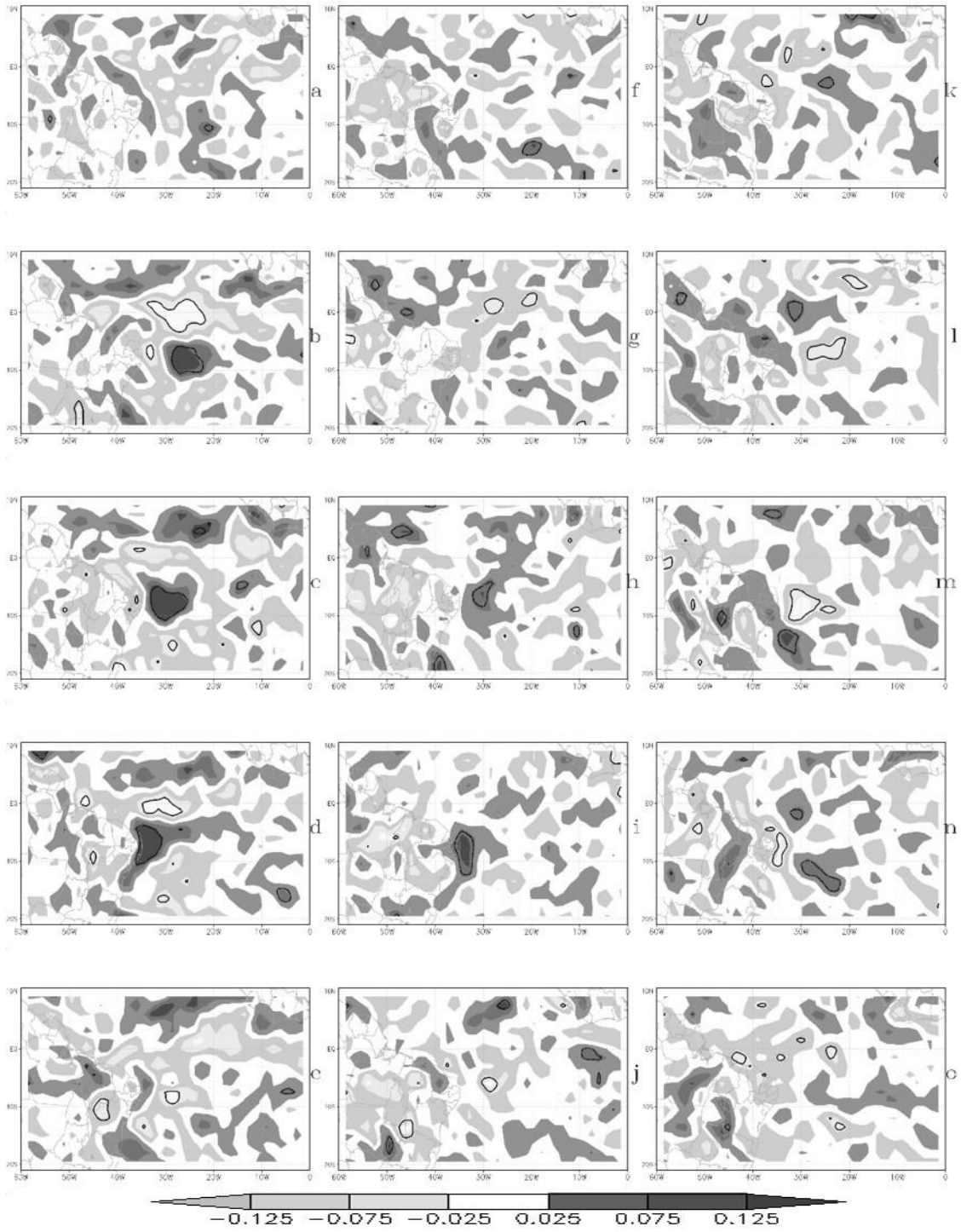

Fig. 5 Divergence (x10-5 s-1, shaded with scale at the bottom) anomalies due EWDs from day -3 (a, f, k), day -2 (b, g, l), day -1 (c, h, m), day 0 (d, i, n) and day +1 (e, j, o) at 1000 (a-e), 850 (f-j) and 700 hPa (k-o). The black line indicates the statistically significant anomalies at 90%.

3.4 EWDs Vertical Structure

The EWDs vertical structure is analyzed through vertical cross sections over the 5ºS-9ºS latitude range (Figs. not shown). These latitudes are used considering the EWDs strength and areas

usually affected over ENEB (see Figs. 4-8 and Yamazaki 1975; Chou 1990; Espinoza 1996; Mota 1997). At 5°S the cross section shows cyclonic vorticity at low levels, from the surface up to 700 hPa, that intensify on day 0 closer to ENEB (~35°W) in the same area where the relative humidity is larger than 70% in the 1000-600 hPa layer. Similar vertical distribution occurs at 9°S, but the variable magnitudes are larger.

Figure 6 shows the anomalies cross sections. The vorticity anomaly in 5°S (Figs. 6a-e) is cyclonic at lower levels, which is the EWDs typical vertical structure (Reed et al. 1977). The opposite occurs in the cross section at 9°S where anticyclonic vorticity anomalies predominate above 900 hPa (Figs. 6f-j). However, as shown in the horizontal fields, the vorticity presents cyclonic and anticyclonic anomalies, respectively, downstream and upstream of the EWDs trough. In the 1000-600 hPa layer it is noted the westward movement of a cyclonic vorticity core, with the maximum anomaly at day 0 near 36°W (Figs. 6a-e). A positive anomaly of relative humidity is also observed practically at the same position of cyclonic vorticity between days -1 and +1 (Figs. 6c-e).

At 9°S the anomalies are in general more intense than in 5°S (Figs. 6f-j). Above the 900 hPa level, there is an anticyclonic vorticity core propagating in phase with the relative humidity positive anomalies (Figs. 6f-j). The centers are moving westward from days -2 until day 0, and it is noted a cyclonic anomalous core downstream of the anticyclonic one (Figs. 6g-i). This figure shows that there is an increase of relative humidity over ENEB during the EWDs propagation. In the layer between 900 and 500 hPa this increase has already occurred on day -2 at 25°W (Fig. 6g), which then moved to ~29°W on day -1 (Fig. 6h), reaching ENEB on day 0 (Fig. 6i). The positive relative humidity anomalous core is also in phase with the anticyclonic relative vorticity core, propagating between day -1 from ~29°W (Fig. 6h) to the ENEB vicinity on day 0 in the 900-500 hPa layer (Fig. 6i).

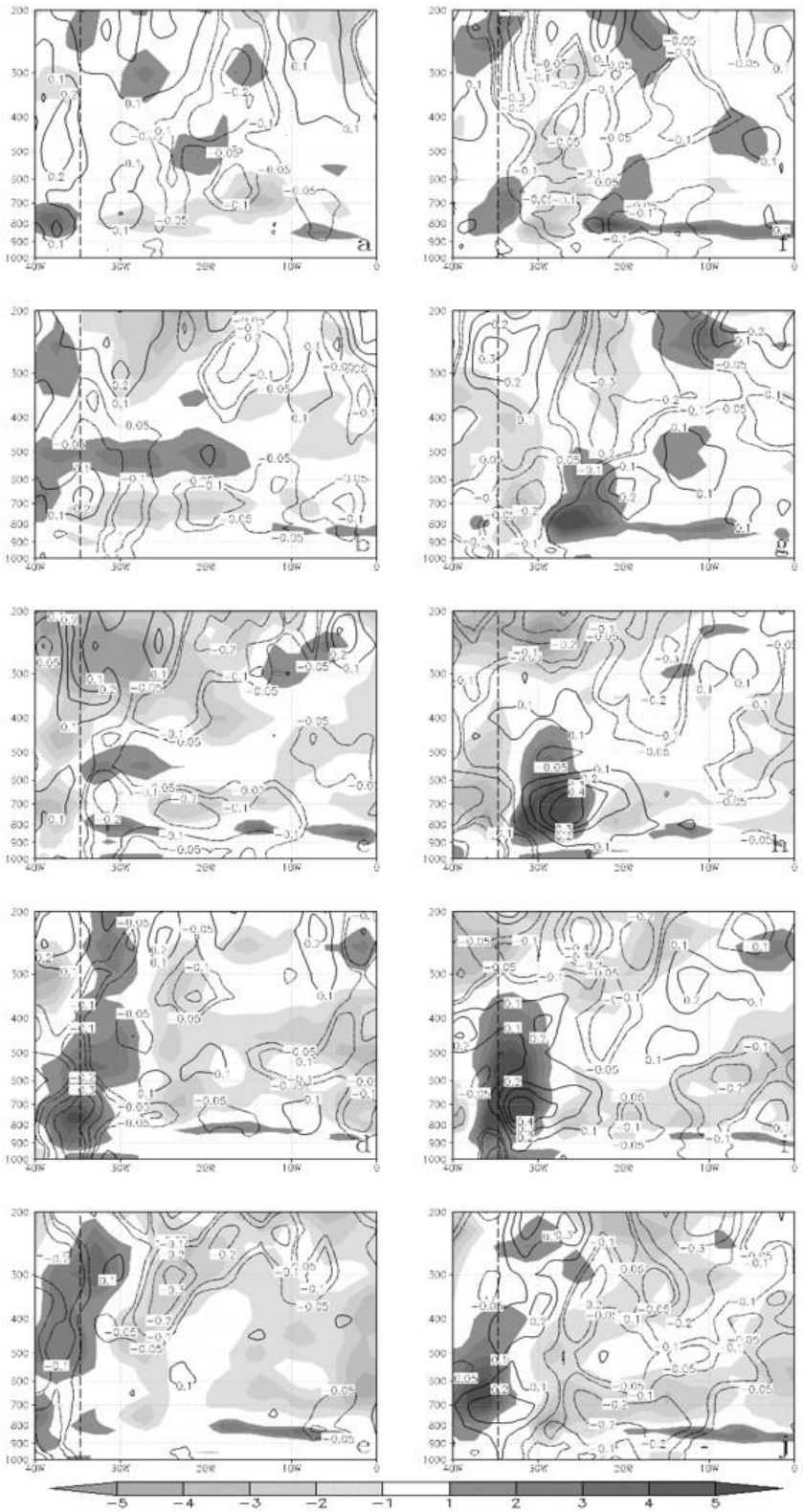

Fig. 6 Composites of relative vorticity (x 10-5 s-1 black lines) and relative humidity (shaded) anomalies during EWDs at 5°S (a-e) and 9°S (f-j) between day -3 (a)-(f), day -2 (b)-(g), day -1 (c)-(h), day 0 (d)-(i) and day +1 (e)-(j). The vertical dashed line marks the ENEB position (around 35°W).

The horizontal wind and omega cross sections help to show the EWDs circulation (Riehl 1979; Hall 1989). Omega and horizontal wind anomalies cross sections at 5°S and 9°S are presented in Figure 7. At 5°S, there is a weak negative omega anomaly at the 700 hPa level on day -2 close to ~22°W (Fig. 7b) that intensifies on day -1 around ~29°W (Fig. 7c). On day 0, the upward anomaly is further intense near the ENEB coast (Figs. 7d). The horizontal wind anomaly shows the trade winds change (southeast to northeast) practically in the same place where omega presents negative anomalous cores. Additionally, at day 0 there are also wind direction changes at middle and upper levels (Fig. 7d). On day +1 it is observed a fast decay of the upward anomaly and a weakening of the wind anomalies (Fig. 7e).

The cross section at 9°S shows a similar westward propagation of the omega negative anomaly cores mainly in the 900-700 hPa layer. At day -2 the upward cell is near 27°W (Fig. 7g), moving to ~30°W on day -1 (Fig. 7h) and finally attains ~35°W on day 0 with maximum intensity (Fig. 7i). As in 5ºS, at 9°S the upward motion weakens on day +1 (Fig. 7j). In general, the upward motion anomalies are stronger at 9°S than at 5°S since day -2 (Fig. 7g). The horizontal wind anomalies at 9°S are similar to that of 5°S.

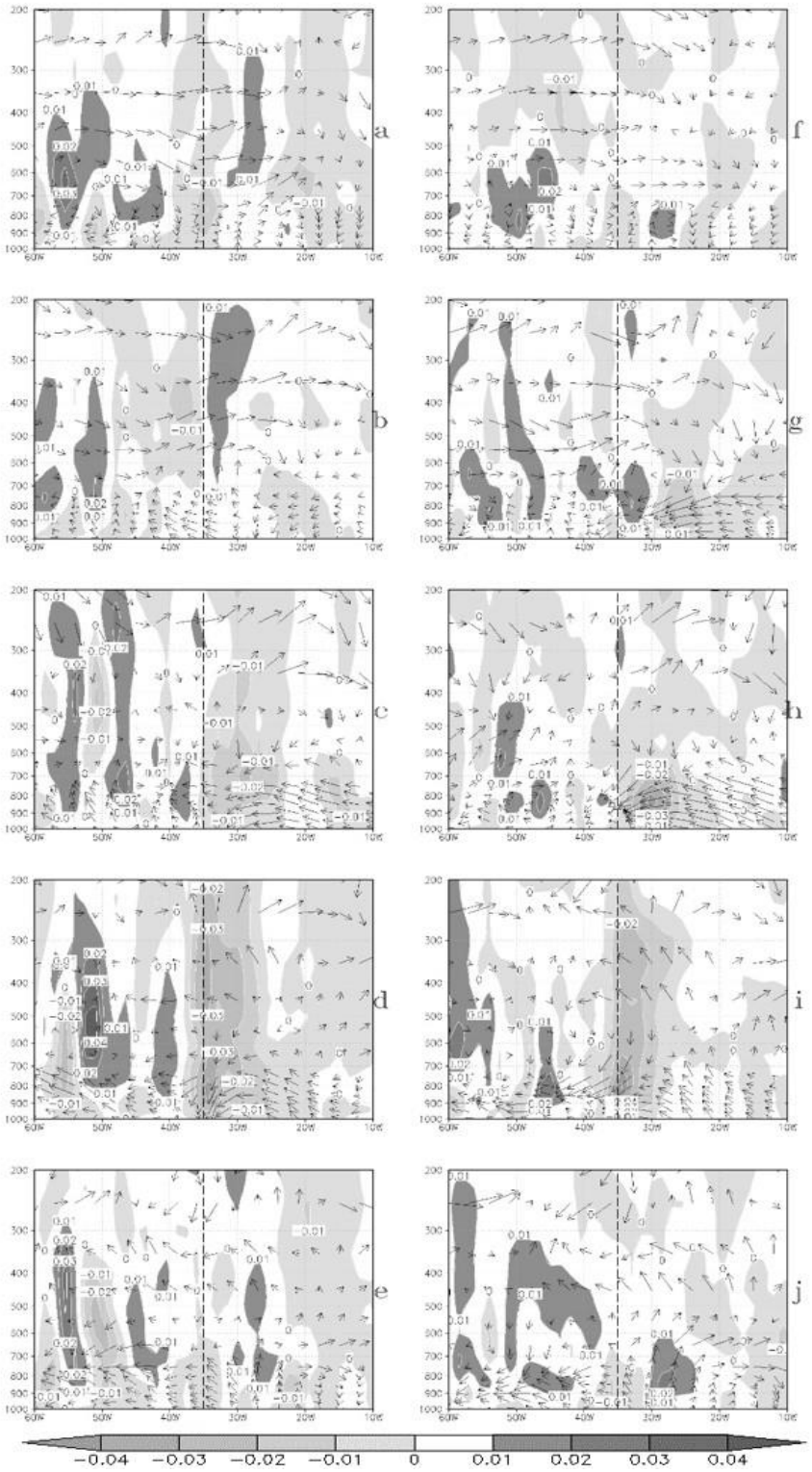

Fig. 7 Composites of wind (arrows) and omega (shaded) anomalies during EWDs at 5°S (a-e) and 9°S (f-j) between day -3 (a)-(f), day -2 (b)-(g), day -1 (c)-(h), day 0 (d)-(i) and day +1 (e)-(j). The vertical dashed line marks the ENEB position (around 35°W).

4. Precipitation and OLR Associated to the EWDs

The precipitation anomalies obtained from TRMM data from day -2 until day +2 indicate the path of the EWDs over TSA (Fig. 8). In all composites days there is an east-west rainfall band over the north Atlantic Ocean (~5ºN) very likely associated at most with ITCZ (Figs. 8a-e). Near ENEB, the rainfall anomaly is negative, with -1/-2 mm day^{-1} on day -2 and day -1 (Figs. 8a-b). Over the ATS, a positive core can be seen spreading from ~7ºS/25ºW at day -2 to ~7ºS/29ºW at day -1 (Figs. 8a-b). However, the precipitation intensifies on day 0 and attains a maximum anomaly core of 6 mm day^{-1} due to EWDs activity over ENEB cost (Fig. 8c). There's almost no precipitation anomalies in SE and over BA coast, indicating that these ENEB areas are less affected by EWDs. The TRMM data show also a positive core of ~1-2 mm day^{-1} over eastern PE, PB and RN on day +1 (Fig. 8d). The anomalies back to negative on day +2 (Fig. 8e).

In order to complement the analysis of the precipitation associated to the EWDs, the OLR is used as a "proxy" for the precipitation occurrence. As shown in Table 2, almost 60% of the detected EWDs are associated with at least moderately convective activity. The composites (Figs. not shown) show lower OLR values in the ITCZ area, where deep convective cloud predominates, and larger OLR values in the region influenced by SASR, where shallow cloudiness occurs.

The absence of an expected EWDs "trail" in the OLR composites may be due to the fact that EWDs cloudiness typically becomes convective as it interacts with local circulations, such as land-sea breezes and topography (Mota 1997). In fact, the infrared satellite images suggest that the EWDs propagation over TSA from Africa leads to the clouds dissipation near the SASR region, which can later regenerate near ENEB, increasing once again the clouds amount when closer to ENEB. In this area, SASR has a lower influence (the trade winds inversion influence is lower), since the subsidence becomes weaker.

Although it is hard to identify EWDs in OLR composites, the OLR composite anomalies show clearly the EWDs signal (Fig. 8f-j). The EWDs stood out in Figures 9f-j, since negative OLR anomalies are propagating around areas of positive anomalies. The OLR negative anomaly due to EWDs is noted since day -2 near ~24°W-8°S (Fig. 8f). From day -1 until day 0 the negative core intensifies and displaces westward (Figs. 8g-h). The OLR minimum occurs on day 0 over ENEB (Fig. 8h), weakening on day +1 (Fig. 8i) and giving place to the OLR positive anomaly over ENEB on day +2 (Fig. 8j). This positive core is present already on days 0 and +1 (Figs. 8h-i), behind the minimum OLR core.

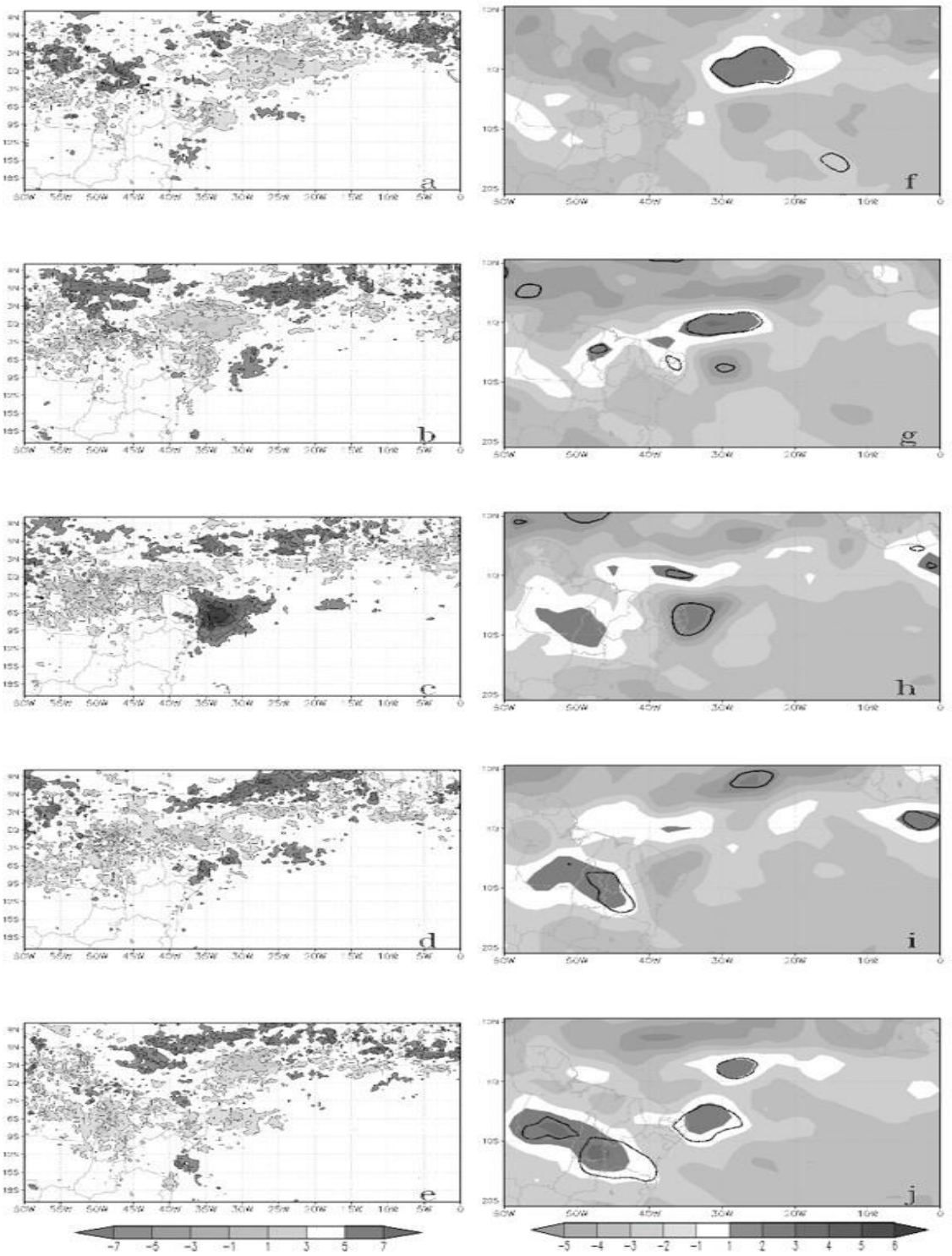

Fig. 8 EWDs anomalies of precipitation (mm day-1 with scale at the bottom) (a)-(e) and outgoing longwave radiation anomalies (W m-2 with scale at the bottom) (f, j) day -2 (a, f), day -1 (b, g), day 0 (c, h), day +1 (d, i) and day +2 (e, j). The black lines in (f-j) indicate the anomalies statistically significant at 90%. *Figures 8f-j seem to indicate that when convection is active (inactive) over ENEB due to EWDs there is significant reduction (increase) of the ITCZ convection in the equatorial region over the ocean and also on the continent over the east-central Amazon.*

For TRMM data, Figure 9 presents the average for the 2006-2007 precipitation associated with EWDs. This EWDs precipitation was estimated by the satellite imagery analysis, being the estimated total rainfall between the arrival and dissipation of the EWDs cloudiness over ENEB. It is worth to remember that each EWDs event cause about 2.6 rainy days (standard deviation of ±1.5 days) (Table 1). According to the TRMM data, during each EW event occurs about 16-20 mm of precipitation between the eastern PE and RN (Fig. 9d) and it is possible to note a northeast-southwest orientation in the EWDs precipitation pattern (Fig. 9b).

The ratio between the total precipitation due to EWDs (Fig. 9b) and total precipitation during rainy season (Fig. 9a) is shown in Figure 10c. This figure shows that EWDs contribute for 70% or more of the total AMJJ precipitation in a narrow area of ENEB, from the coast of AL to the eastern RN (Fig. 9c). Furthermore, the TRMM data indicates that EWDs accounts for 60% of the AMJJ rainfall between eastern AL and the central part of RN. The EWDs contribution to the AMJJ rainfall is smaller over the southern ENEB, including the eastern BA. In terms of daily intensity, during each EW event it is observed on average 16-20 mm of precipitation from eastern PE to eastern RN.

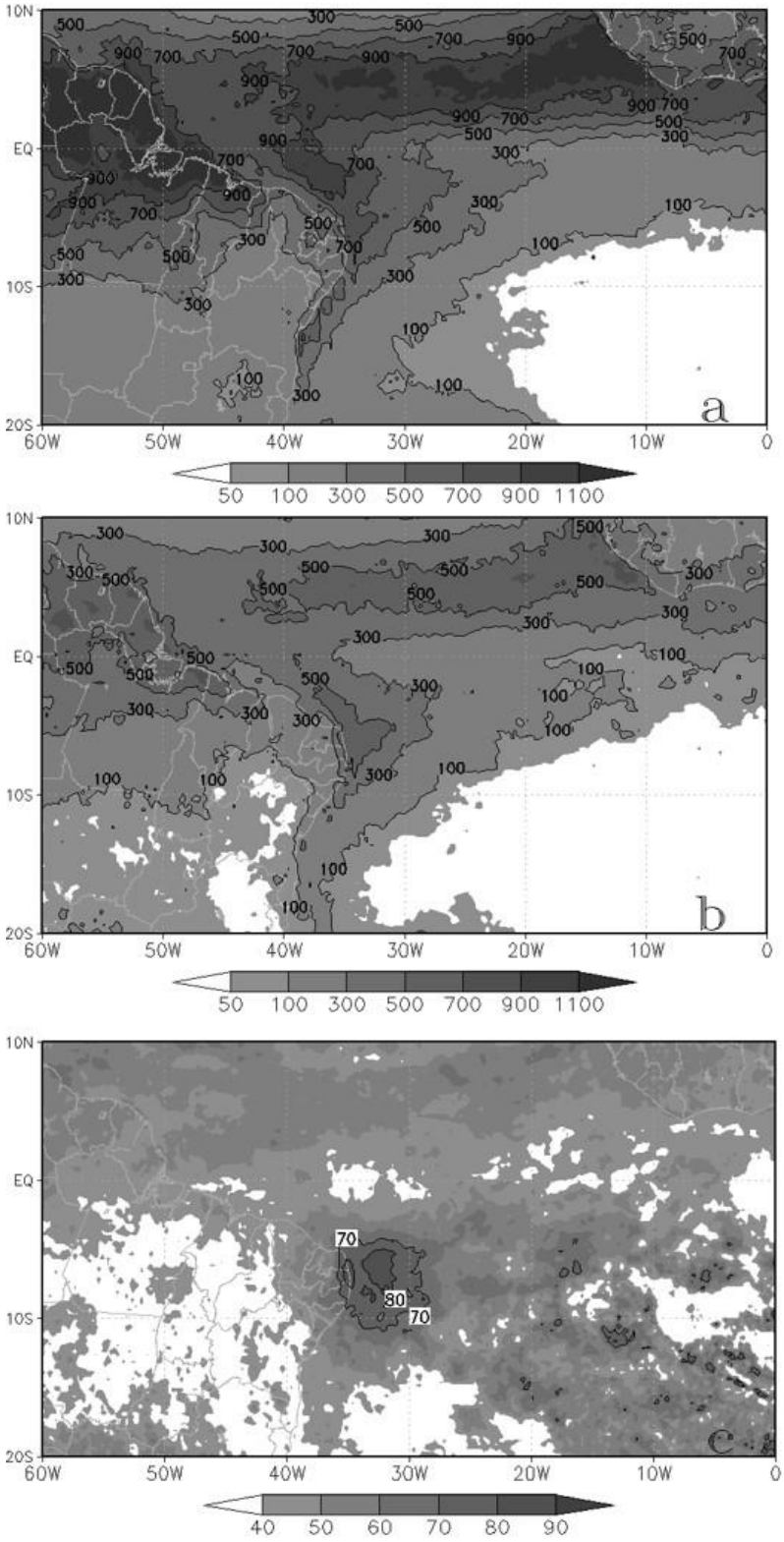

Fig. 9 2006-2010 AMJJ climatology of precipitation (mm) (a), EWDs mean precipitation (mm) (b), ratio (%) between climatology and EWDs mean precipitation contribution (c).

5. Conclusion and Remarks

For the AMJJ period from 2006-2010 the subjective analysis identified a total of 116 EWDs propagating over TSA and reaching ENEB. In approximately 90% of the events it was observed a trough at 700 hPa associated with the EWDs, indicating that the analysis of the circulation at this level is important to locate and track these systems. On average, 23 EWDs are observed per rainy season with small interannual variability. These waves have on average a period of 5.3 days, wavelength of 4307 km and phase speed of 9.5 m s^{-1}.

The Hovmöller diagrams could determine by itself ~68% of the EWDs that were subjectively obtained from satellite imagery and reanalysis. This indicates some limitation of the Hovmöller diagram to be used as an objective technique to identify EWDs in this region.

The EWDs composites show an organized structure at low levels, especially in the anomalous circulations at 1000 hPa. The anomalies during EWDs propagation presents a confluent, cyclonic relative vorticity and convergence from two days before until the day that they wave arrive in ENEB. The EWDs propagation is also clear in the OLR field, where negative OLR anomalies (indicating clouds and precipitation) may be followed since two days before until one day after EWDs arrival in ENEB. The anomalous fields suggest that the EWDs have better organized structure in both vorticity and circulation anomalies at 1000 and 850 hPa. This is a new result to the TSA EWDs, since previous studies did not consider their identification at the 1000 hPa level.

The vertical cross sections of the relative humidity and pseudo-vertical velocity show anomalous cores of moist and upward motion propagating with EWDs since two days before until the day that they reach ENEB. For the relative vorticity, it is observed a strong dependence with latitude, but there is some similarities to that reported in the literature (Reed and Reck 1971; Tai and Ogura 1986; Mota 1998; Alves et al. 2006): EWDs present cyclonic vorticity near the trough axis at low and mid levels and anticyclonic vorticity at upper levels. At 5°S the cyclonic anomaly is observed in the 1000-700 hPa layer, but at 9°S there is an anticyclonic anomaly already at 900 hPa, extending to ~500 hPa.

The composites also show positive anomalies of precipitation persisting until one day after the arrival of the EWDs on ENEB. For the AMJJ months, the EWDs are responsible for 70% or more of the total rainfall between the AL northern coast and eastern RN. In other ENEB areas (SE and other areas of RN) these systems may produce at least half of the seasonal precipitation. This indicates the great importance of the EWDs to the rainy season of ENEB, as suggested in previous

works (Yamazaki and Rao 1977; Chou 1990; Espinoza 1996; Mota 1997).

An extension of the present work would consider applying EWDs identification technique, tracking and composition to a larger period to obtain a long-term climatology of the EWDs affecting ENEB. This initial step (case dates establishment) is observational and represents an analysis that requires much time. Therefore, the use of an objective methodology would greatly facilitate EWDs identification. In this process the satellite imagery would be essential, since these waves always have some related cloud cover, even if weak and very irregular along its path. In fact, the result of tracking techniques can be applied to regional models data thus evaluating their skill in the TSA EWDs prediction/simulation.

Acknowledgments - The authors were supported by CNPq and CAPES-PROEX. We also want to thank the ECMWF, TRMM, NOAA and CPTEC/INPE for providing the datasets which are available in public domain.

6. References

Alves, MAS, Oyama MD and Yamazaki J. Composição de Ventos de Distúrbios Ondulatórios de Leste sobre as Regiões de Alcântara e Natal: Caracterização Preliminar. *XIV Congresso Brasileiro de Meteorologia, Florianópolis*. 2006.

Asnani GC (1993) Tropical Meteorology. In: Easterly Waves. Pashan, India. 1202p.

Burpee RW (1974). Characteristics of North African easterly waves during the summers of 1968 and 1969. *Journal of the Atmospheric Sciences*, 31(6), 1556-1570.

Céron JP, JF Guérémy 1999. Validation Of The Space–Time Variability Of African Easterly Waves Simulated By The CNRM GCM. *J. Climate*, 12, 2831–2855.

Chang CP and Miller CR 1977. Comparison Of Easterly Waves In The Tropical Pacific During Two Contrasting Periods Of Sea-Surface Temperature Anomalies. *J. Atmos. Sci.*, 34, 615- 28.

Chan CS (1990) Análise de distúrbios ondulatórios de leste sobre o Oceano Atlântico Equatorial Sul. Dissertation, Instituto Nacional de Pesquisas Espaciais.

Da Rocha RP, Rodrigues CAM, Cuadra SV and Ambrizzi T (2009). Precipitation diurnal cycle and summer climatology assessment over South America: An evaluation of Regional Climate Model version 3 simulations. *Journal of Geophysical Research*, v. 114, p. 1-19. (doi: 10.1029/2008JD010212).

Dee, DP et al. 2011. The Era-Interim Reanalysis: Configuration And Performance Of The Data Assimilation System. *Quarterly Journal Of The Royal Meteorological Society*. 137:656, 553-597.

Espinoza ES (1996) Distúrbios Nos Ventos De Leste No Atlântico Tropical. Dissertation, Instituto Nacional De Pesquisas Espaciais.

Fedorova N (2008). Sinótica III: Frentes, Correntes De Jato, Ciclones e Anticiclones. In: Anticiclones. Maceió, Alagoas.

Gomes, HB; Ambrizzi, T; Pontes Da Silva, BF; Hodges, K; Silva Dias, PL; Herdies, DL; Silva, MCL; Gomes, HB. Climatology of easterly wave disturbances over the tropical South Atlantic. *Climate Dynamics*, v. 51, p. 1-19, 2019.

Hall, BA. Westward-Moving Disturbances In The South Atlantic Coinciding With Heavy Rainfall Events At Ascension Island. 1989. *Meteorology Magazine*, V.118, P.175-181, 1989.

Huffman, GJ, Adler RF, Bolvin DT, Gu G, Nelkin EJ, Bowman KP, Stocker EF, Wolff DB (2007) The TRMM Multi-Satellite Precipitation Analysis: Quasi-Global, Multi-Year, Combined-Sensor Precipitation Estimates At Fine Scale. *J. Hydrometeor*., 8, 33-55.

Keshavamurty RN (1971) Vertical Coupling In The Indian Summer Monsoon. *Nature Physical Science* 232, 169-170.

Kouadio YK, Servain J, Machado LAT and Lentini CAD (2012) Heavy Rainfall Episodes In The Eastern Northeast Brazil Linked To Large-Scale Ocean-Atmosphere Conditions In The Tropical Atlantic. *Advances In Meteorology*, Article Id 369567, 16 Pages, 2012. Doi:10.1155/2012/369567.

Kousky VE (1980) Diurnal Rainfall Variation In Northeast Brazil. *Mon. Weather Rev*, 108, 488-498.

Kousky VE (1979) Frontal Influences On Northeast Brazil. *Mon. Wea. Rev.*, 107, 1142-1153.

Krishnamurti TN, Baumhefner D (1966) Structure Of A Tropical Disturbance Based On Solutions Of A Multilevel Baroclinic Model. *Journal Of Applied Meteorology*, Vol. **5**, Issue 4, Pp.396-406.

Merritt ES (1964) Easterly Waves And Perturbations: A Reappraisal. *Journal Of Applied Meteorology*, 3:367-382.

Molion LCB and Bernardo SO (2002) Uma Revisão Da Dinâmica Das Chuvas No Nordeste Brasileiro. *Revista Brasileira De Meteorologia*, V.17, N.1, P. 1-10.

Mota GV (1997) Estudo Observacional De Distúrbios Ondulatórios De Leste No Nordeste Brasileiro. Dissertation, University of Sao Paulo.

Mota GV and Gandu AW (1996) Análise de Distúrbios Ondulatórios de Leste que Afetam o Nordeste Brasileiro: Um Estudo De Caso. *IX Congresso Brasileiro De Meteorologia*.

Mota GV and Gandu AW (1998) Análise Dos Padrões Ondulatórios De Leste No Nordeste Brasileiro Durante O Inverno De 1994. *X Congresso Brasileiro De Meteorologia*, Brasília.

Neiva EJF (1975) An Investigation Of Wave-Type Disturbances Over The Tropical South-Atlantic. Dissertation, Naval Post Graduate School, Monterrey, California.

Philander SG (1990) El Niño, La Niña, And The Southern Oscillation. *Academic Press, International Geophysics Series*, Vol. 46.

Pontes da Silva BF (2008) Sistemas Sinóticos Associados Às Precipitações Intensas No Estado De Alagoas. Maceió, pp 149. Trabalho De Conclusão De Curso – Instituto De Ciências Atmosféricas, Universidade Federal De Alagoas.

Pontes da Silva BF, Fedorova N, Levit V, Peresetsky A And Brito BM (2011) Sistemas Sinóticos Associados Às Precipitações Intensas No Estado De Alagoas. *Revista Brasileira De Meteorologia*, V.26, N.3, pp 323 - 338.

Reed JR and Recker EE (1971) Structure And Properties Of Synoptic-Scale Wave Disturbances In The Equatorial Western Pacific. *J. Atmos. Sci.*, 28, pp 1117-1133.

Reed RJ, Norquist DC and Recker EE (1977) The Structure And Properties Of African Wave Disturbances As Observed During Phase III Of Gate. *Mon. Wea. Rev.* 105, pp 317–333.

Riehl H (1979) Climate And Weather In The Tropics. London: *Academic Press*. XII + 611 Pp.

Riehl H (1945) Waves In The Easterlies And The Polar Front In The Tropics, Chicago: University Of Chicago Press, 79p.

Rosenthal SL (1960) A Simplified Linear Theory Of Equatorial Easterly Waves. *J. Meteor*., 17, pp 484–488. Doi: Http://Dx.Doi.Org/10.1175/1520-0469(1960)017<0484:Asltoe>2.0.Co;2.

Shapiro LJ (1977) Tropical Storm Formation From Easterly Waves: A Criterion For Development. *J. Atmos. Sci.*, 34(7), pp 1007-1021.

Tai KS and Ogura Y (1987) An Observational Study Of Easterly Waves Over The Eastern Pacific In The Northern Summer Using FGEE Data. *Journal Of The Atmospheric Sciences*, 44(2):pp 339-361.

Thorncroft C and Hodges K (2001) African Easterly Wave Variability And Its Relationship To Atlantic Tropical Cyclone Activity, *J. Clim.*, v. 14, pp 1166-1179.

Uvo CRB and Nobre CA (1989) A Zona De Convergência Intertropical (ZCIT) e a Precipitação No Norte Do Nordeste Do Brasil. Parte I: A Posição Da ZCIT No Atlântico Equatorial. *Climanálise*, Vol. 4, N 07, pp 34-40.

Wilks DS (2006) Statistical Methods In The Atmospheric Sciences. Ed. 2nd, *Academic Press San Diego*, 467p.

Williams KT (1970) Characteristics Of The Wind, Thermal, And Moisture Fields Surroundings The Satellite-Observed Mesoscale Trade Wind Cloud Clusters In The Western North Pacific. Preprints Of Papers, Symp. Tropical Meteorology, Honolulu, *Amer. Meteor. Soc.*, D Iv-1 A D Iv-6.

Yamazaki Y and Rao VB (1977) Tropical Cloudiness Over The South Atlantic Ocean, *Journal Of The Meteorological Society Of Japan*, 55(2), pp 205-207.

Yamazaki Y (1975) Estudos Teóricos E Sinóticos Dos Distúrbios Tropicais. Dissertation, Instituto Nacional de Pesquisas Espaciais.

Yanai M (1963) A Preliminary Survey Of Large-Scale Disturbances Over The Tropical Pacific Region. *Geofis. Int.*, 3, pp 73–84.

Yanai M (1968) Evolution of a Tropical Disturbance in the Caribbean Sea Region. *J. Of The Meteorol. Soc. Of Japan*, 46, pp 86-109.

Data do envio: 05 de agosto de 2020
Data do aceite: 10 de maio de 2021
Data da publicação em ahead of print: 10 de maio de 2021

Como citar:
SILVA, Bruce Francisco Pontes da; ROCHA, Rosmeri Porfírio da; GOMES, Helber Barros. Easterly Wave Disturbances Activity Over the Eastern Northeast Brazil During 2006-2010 Rainy Seasons. **Revista Cientifica Foz,** São Mateus, Espírito Santo v.3 n.2, p. 203-232, ago/dez, 2020. Disponível em:_____. Acesso em:____.